

Dielectric functions of Si nanocrystals embedded in a SiO₂ matrix

T. P. Chen,* Y. Liu, M. S. Tse, O. K. Tan, P. F. Ho, and K. Y. Liu

School of Electrical and Electronic Engineering, Nanyang Technological University, Singapore 639798

D. Gui

Institute of Microelectronics, Singapore Science Park II, Singapore 117685

A. L. K. Tan

Singapore Institute of Manufacturing Technology, Singapore 638075

(Received 22 May 2003; published 7 October 2003)

Knowing the dielectric functions of semiconductor nanocrystals isolated in a dielectric matrix is important to both solid-state physics and applications. In this work, we have developed an approach to determine the dielectric function of Si nanocrystals embedded in a SiO₂ matrix synthesized with Si ion beams. The approach is based on the effective medium approximation, and appropriate models are developed to simulate the secondary ion mass spectroscopy and spectroscopic ellipsometry measurements on the material system. The energy gap expansion of the Si nanocrystals due to the nanocrystal size effect has been obtained by modeling the real part of the dielectric function with the single-oscillator model. From the energy gap expansion, the nanocrystal size can be also obtained with two independent models including the phenomenological model based on quantum confinement and the bond contraction model. The results from the two models are similar and are also consistent with transmission electron microscope and x-ray diffraction measurements.

DOI: 10.1103/PhysRevB.68.153301

PACS number(s): 78.20.Ci, 78.67.Bf

In recent years, a great deal of research on Si nanocrystals (nc-Si) embedded in a SiO₂ matrix has been conducted due to their potential applications in Si-based optoelectronic devices and single-electron memory devices or other single-electron devices.¹⁻⁶ One of the promising techniques being used to elaborate nc-Si is the implantation of Si ions into robust SiO₂ thin films that provide good chemical and electrical passivation of the nanocrystals. This synthesis process yields a narrow-size distribution of nanocrystals, and it is fully compatible with the mainstream complementary metal-oxide-semiconductor (CMOS) process. For Si nanocrystals embedded in a SiO₂ matrix, their optical and dielectric properties should be different from those of bulk crystalline Si due to the size effect, and as the Si nanocrystals are isolated by the SiO₂ matrix the situation should be also different from that of a continued Si-nanocrystal film. Therefore, it would be interesting to examine the properties of the isolated nanocrystals embedded in a SiO₂ matrix, and knowing the dielectric function of the nanocrystals isolated in a SiO₂ matrix is definitely important to both solid-state physics and applications. In this work, the dielectric function and optical constants of Si nanocrystals embedded in a SiO₂ matrix are determined, and from these results the energy gap expansion of the nanocrystals due to the size effect is obtained. In addition, the nanocrystal sizes can also be estimated from the energy gap expansion, and the result is consistent with high-resolution transmission electron microscope (HRTEM) and x-ray diffraction (XRD) measurements.

550-nm-thick SiO₂ films were grown on *p*-type Si (100) substrates by wet oxidation of Si at 1000 °C. The SiO₂ films were implanted with a dose of 1×10^{17} atoms/cm² of Si⁺ at 100 keV. The samples were annealed at 1000 °C in nitrogen gas for a duration of 20 min. Upon such an annealing, one would expect the formation of Si nanocrystals in the SiO₂

film.^{7,8} Figure 1(a) shows the HRTEM image of nc-Si embedded in a SiO₂ matrix. The mean size of the Si nanocrystals could be determined from the full width of half maximum (FWHM) of the Bragg peak after correction for instrumental broadening in the XRD measurement.⁹ Figure 1(b) shows the XRD measurement for nc-Si embedded in a SiO₂ matrix and the pseudo-Voigt fit to the data, and the nc-Si size obtained is ~ 4.6 nm. The depth distribution of Si nanocrystals in SiO₂ film was obtained from secondary ion mass spectroscopy (SIMS) measurements. Spectroscopic ellipsometry measurements were carried out to determine the ellipsometric angles Ψ and Δ in the wavelength range of 400–1200 nm.

The volume fraction of Si nanocrystals in SiO₂ film as a function of depth was calculated from the SIMS measurement, and the result is shown in Fig. 2. As can be seen in Fig. 2, nc-Si distributes from the surface to a depth of 250 nm, and there are few or no nanocrystals in the SiO₂ film beyond a depth of 250 nm. Therefore, the SiO₂ film can be approximately represented by the two layers: i.e., the first layer ($0 \leq \text{depth} \leq 250$ nm), which contains Si nanocrystals, and the second layer ($\text{depth} > 250$ nm), which is basically a pure SiO₂ layer. For the first layer, as the volume fraction of Si nanocrystals varies with depth; the optical properties in this layer will also vary with depth. To model the optical properties of the first layer, it is divided into m sublayers with equal thickness d_0 ($m = 25$ and $d_0 = 10$ nm in this study), namely, sublayer 1, sublayer 2, ..., sublayer m in the sequence starting from the surface, and the volume fraction of Si nanocrystals is considered constant within each sublayer. Each sublayer has its own complex refractive index $N_i = n_i + jk_i$ ($i = 1, 2, \dots, m$) where n_i and k_i are the refractive index and extinction coefficient for the i th sublayer, respectively. Note that N_i is also a function of wavelength (λ). Therefore, in the

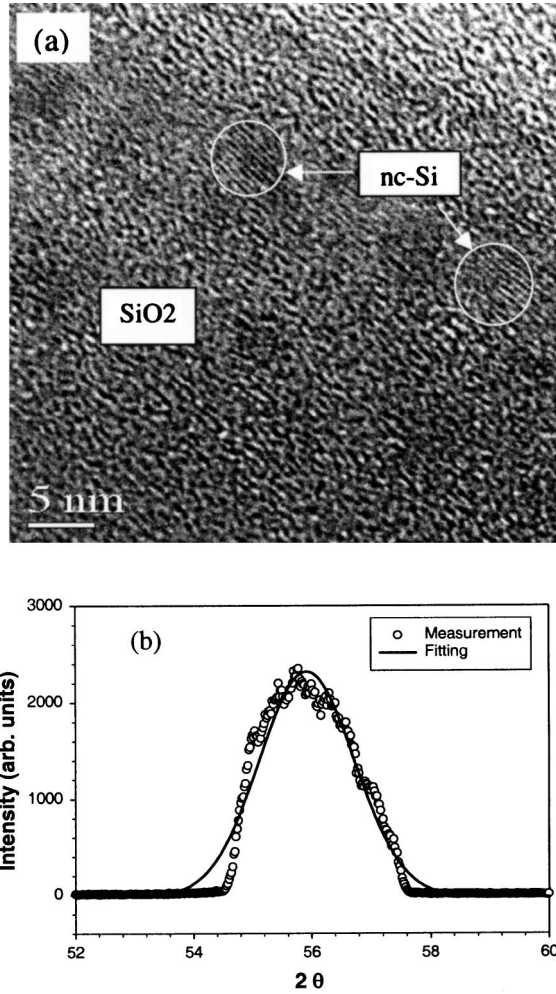


FIG. 1. (a) HRTEM image of nc-Si embedded in a SiO_2 matrix and (b) XRD measurement for nc-Si embedded in a SiO_2 matrix and the pseudo-Voigt fit to the data.

ellipsometry analysis, the material system used in this study can be described by a $(m+3)$ -phase model, i.e., air/sublayer 1/ \dots /sublayer m /pure SiO_2 layer (i.e., the second layer mentioned above)/Si substrate. Each phase is characterized by its complex refractive index N_i ($i=0,1,\dots,m,m+1,m+2$). Note

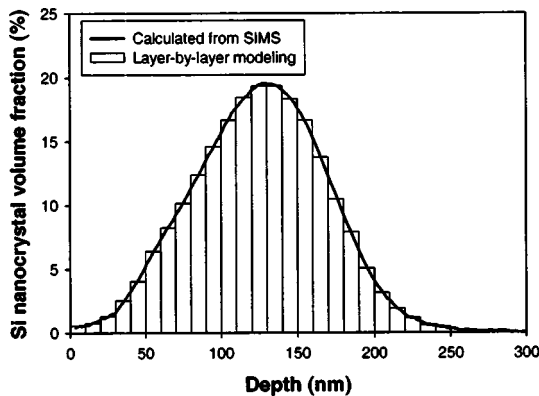


FIG. 2. Volume fraction of Si nanocrystals embedded in SiO_2 film vs depth.

that $N_0=1$ for air, $N_{m+1}=N_{\text{SiO}_2}$ (i.e., the SiO_2 complex refractive index) for the pure SiO_2 layer, and $N_{m+2}=N_{\text{Si}}$ (i.e., the Si complex refractive index) for the Si substrate. As N_0 , N_{m+1} , and N_{m+2} are known, for a fixed incident angle ϕ_0 the ellipsometric angles ψ and Δ can be expressed as functions of the parameters N_1, N_2, \dots, N_m , and λ (Refs. 10 and 11), i.e.,

$$\psi = f_1(N_1, N_2, \dots, N_m, \lambda) \quad (1)$$

and

$$\Delta = f_2(N_1, N_2, \dots, N_m, \lambda). \quad (2)$$

Note that the functions f_1 and f_2 cannot be expressed as analytical formulas as they are very complicated for such a $(m+3)$ -phase system (here $m=25$).

For the first layer mentioned above, it can be treated as a material system in which the SiO_2 is a host material while the Si nanocrystal is an inclusion embedded in the host material. Although the Si nanocrystal fraction varies with the depth and there may be a size distribution for the nanocrystals, for each sublayer of the first layer, its effective complex dielectric function ε_i ($=N_i^2, i=1,2,\dots,m$) can be calculated with the following effective medium approximation:^{10,12}

$$\frac{\varepsilon_i - \varepsilon_{\text{SiO}_2}}{\varepsilon_i + 2\varepsilon_{\text{SiO}_2}} = \nu_i \frac{\varepsilon_{\text{nc-Si}} - \varepsilon_{\text{SiO}_2}}{\varepsilon_{\text{nc-Si}} + 2\varepsilon_{\text{SiO}_2}}, \quad (3)$$

where ν_i ($i=1,2,\dots,m$) is the volume fraction of the nanocrystals in the i th sublayer, $\varepsilon_{\text{SiO}_2}$ is the dielectric function of host material SiO_2 , and $\varepsilon_{\text{nc-Si}}$ is the dielectric function of the Si nanocrystal. Here the nanocrystal size distribution is considered in terms of the mean dielectric function. As the volume fraction (ν_i) and $\varepsilon_{\text{SiO}_2}$ are known, from Eq. (3) the effective complex dielectric function ε_i (and thus the complex refractive index N_i) for the i th sublayer ($i=1,2,\dots,m$) can be expressed in terms of $\varepsilon_{\text{nc-Si}}$ (or the complex refractive index of nc-Si, i.e., $N_{\text{nc-Si}}$). Therefore, Eqs. (1) and (2) can be rewritten in the form of

$$\psi = f'_1(N_{\text{nc-Si}}, \lambda) \quad (4)$$

and

$$\Delta = f'_2(N_{\text{nc-Si}}, \lambda). \quad (5)$$

Again the functions f'_1 and f'_2 cannot be expressed as analytical formulas as they are very complicated. For a given wavelength λ , an ellipsometric measurement yields a value of Ψ and Δ , and therefore $N_{\text{nc-Si}}$ can be obtained by solving Eqs. (4) and (5). In this study, we use a spectral fitting in the wavelength range from 400 to 1200 nm to determine the $N_{\text{nc-Si}}$ at each wavelength instead of solving the equations. The spectral fitting can avoid the problems of unstable or unreasonable values and difficulties associated with the peak structures of the measured $\Psi(\lambda)$ and $\Delta(\lambda)$ due to the measurement, model, and calculation errors. Figure 3 shows the spectral fitting, i.e., the comparison of the calculated Ψ and Δ based on Eqs. (4) and (5) with the measured Ψ and Δ in

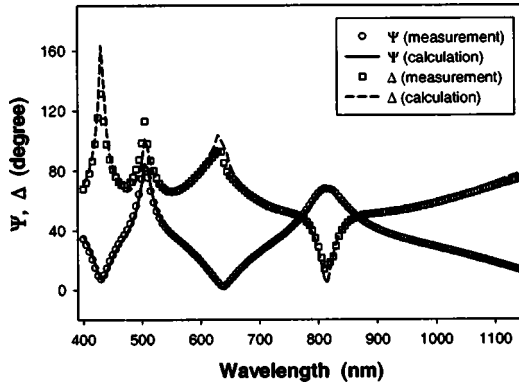


FIG. 3. ψ and Δ as functions of wavelength. The lines represent the best fit with the approach described in the text.

the wavelength range from 400 to 1200 nm. As can be seen in this figure, all the complicated spectral features of both Ψ and Δ can be fitted excellently. This indicates that the above approach is correct and the fitting is effective. The complex refractive index N_{nc-Si} (and thus the refractive index n and extinction coefficient k) of Si nanocrystals embedded in a SiO_2 matrix obtained as a function of wavelength is shown in Fig. 4. The real and imaginary parts of the complex dielectric function of nc-Si obtained are also shown in Figs. 5 and 6, respectively.

As can be seen in Figs. 4–6, the optical constants and dielectric function of the Si nanocrystals are reduced significantly compared to those of bulk crystalline Si. Here the reduction in the optical constants or the dielectric function is attributed to the energy gap expansion of the nanocrystals as a result of the nanocrystal size effect. Based on the single-oscillator model, the change ($\Delta\epsilon_r$) of the real part of the dielectric function due to the energy gap change (ΔE_g) can be expressed as follows for a small energy gap change (i.e., $\Delta E_g/E_{g0} \ll 1$):

$$\frac{\Delta\epsilon_r}{\epsilon_{r0}} = -\frac{2(1-\epsilon_{r0}^{-1})}{1-(E/E_{g0})^2} \left(\frac{\Delta E_g}{E_{g0}} \right), \quad (6)$$

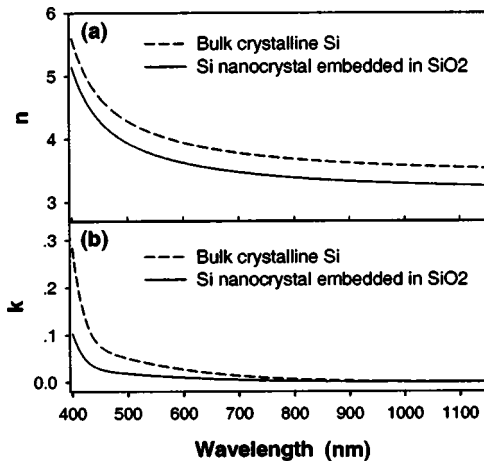


FIG. 4. Refractive index (n) and extinction coefficient (k) of Si nanocrystals embedded in a SiO_2 matrix as functions of wavelength.

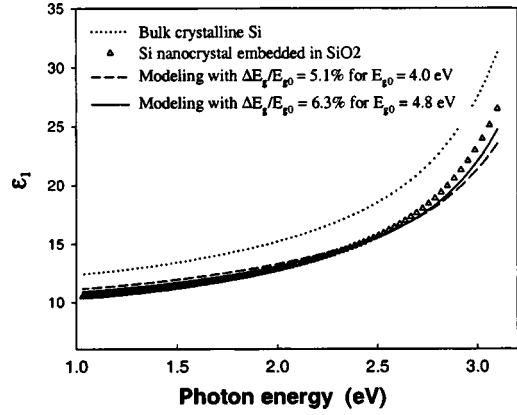


FIG. 5. Real part of the dielectric function of Si nanocrystals embedded in a SiO_2 matrix as a function of wavelength. The modeling with Eq. (6) yields an energy gap expansion of 5.1% and 6.3% for $E_{g0} = 4$ eV and 4.8 eV, respectively.

where ϵ_{r0} and E_{g0} are the real part of dielectric function and energy gap of bulk crystalline Si, and E is the photon energy. Note that the energy gap $E_g (= \hbar\omega_g$ where ω_g is the resonance frequency of the oscillator) in the single-oscillator model is not the same as the fundamental energy band gap of silicon. Tsu *et al.* pointed out that the fundamental Γ - Δ gap at 1.1 eV plays almost no role in the dielectric function.¹³ The energy gap E_{g0} for the dielectric function of bulk crystalline Si was set to be 4 eV in Ref. 13 while it was shown to be 4.8 eV in Ref. 14. In this study, Eq. (6) is used to model the real part of the dielectric function of Si nanocrystals embedded in a SiO_2 matrix, and the result is shown in Fig. 5. The model yields an energy gap expansion of 5.1% and 6.3% for $E_{g0} = 4$ eV and 4.8 eV, respectively.

The nanocrystal size could be estimated from the energy gap change by using the bond contraction model¹⁵ or the phenomenological model based on quantum confinement¹⁶ on the size dependence of energy gap expansion. From the bond contraction model,¹⁵ if the surface bond contraction is significant for only the two outermost atomic layers of a spherical dot and the dot size (i.e., the diameter D) is much larger than the atomic diameter d , the energy gap expansion is given as

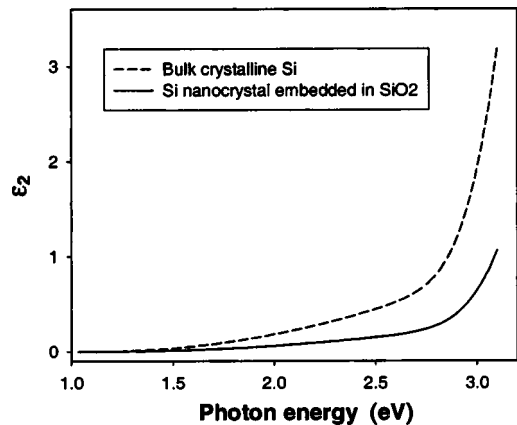


FIG. 6. Imaginary part of the dielectric function of Si nanocrystals embedded in a SiO_2 matrix as a function of wavelength.

$$\frac{\Delta E_g}{E_{g0}} = \gamma'_1 c_1 (c_1^{-m} - 1) + \gamma'_2 c_2 (c_2^{-m} - 1), \quad (7)$$

where

$$\gamma'_i = \frac{3}{k} \left(1 - \frac{i-0.5}{k} \right)^2 \quad (i=1,2),$$

$k = D/(2a)$, $m = 1$, $c_1 = 0.88$, and $c_2 = 0.94$ (Ref. 15). For $\Delta E_g/E_{g0} = 5.1\%$ which corresponds to $E_{g0} = 4$ eV, Eq. (7) yields the nanocrystal size $D = 4.1$ nm, and for $\Delta E_g/E_{g0} = 6.3\%$ which corresponds to $E_{g0} = 4.8$ eV, Eq. (7) yields the nanocrystal size $D = 3.1$ nm. On the other hand, from the phenomenological model,¹⁶ which predicts the trend for quantum confinement—i.e., the inverse dependence of the expanded energy gap on the nanocrystal size—and in which a log-normal distribution of nanocrystal sizes is considered, ΔE_g is given by

$$\Delta E_g = \frac{C}{d_0^n} \left(\frac{d_m}{d_0} \right)^{n(2n+5)/3}, \quad (8)$$

where d_0 (in nm) is the mean size of nanocrystals and d_m is the size for which the maximum occurs in the log-normal distribution, $n = 1.22$, $C = 3.9$, and $d_m/d_0 = 0.7$ (Ref. 16). For

$\Delta E_g/E_{g0} = 5.1\%$, Eq. (8) yields the nanocrystal size $d_0 = 4.7$ nm, and for $\Delta E_g/E_{g0} = 6.3\%$, Eq. (8) yields $d_0 = 3.4$ nm. Obviously, the two models give similar results. These results are close to the value (~ 4.6 nm) obtained from XRD measurements shown in Fig. 1, and they also agree with the result reported in Ref. 7 for similar nc-Si formation conditions.

In summary, we have developed an approach to determine the dielectric function of nc-Si embedded in a SiO₂ matrix synthesized with Si ion implantation. The approach is based on the effective medium approximation, and appropriate models are developed to simulate the nc-Si depth profiles obtained from the SIMS measurement and the ellipsometric parameters measured in a wide range of wavelengths. The energy gap expansion of the nc-Si due to the size effect has been obtained by modeling the real part of the dielectric function with the single-oscillator model. From the energy gap expansion, the nanocrystal size can be also obtained with two independent models including the phenomenological model based on quantum confinement and the bond contraction model. The results from the two models are similar and are also consistent with the HRTEM and XRD measurements.

*Electronic address: echentp@ntu.edu.sg

¹N. Lalic and J. Linnros, *J. Lumin.* **80**, 263 (1999).

²E. Kapetanakis, P. Normand, D. Tsoukalas, and K. Beltsios, *Appl. Phys. Lett.* **80**, 2794 (2002).

³S. Tiwari, F. Rana, H. Hanafi, A. Hartstein, E. F. Crabbé, and K. Chan, *Appl. Phys. Lett.* **68**, 1377 (1996).

⁴E. Kapetanakis, P. Normand, D. Tsoukalas, K. Beltsios, J. Stoenenos, S. Zhang, and J. van den Berg, *Appl. Phys. Lett.* **77**, 3450 (2000).

⁵E. A. Boer, M. L. Brongersma, H. A. Atwater, R. C. Flagan, and L. D. Bell, *Appl. Phys. Lett.* **79**, 791 (2001).

⁶S.-H. Choi and R. G. Elliman, *Appl. Phys. Lett.* **75**, 968 (1999).

⁷B. Garrido, M. López, O. González, A. Pérez-Rodríguez, J. R. Morante, and C. Bonafos, *Appl. Phys. Lett.* **77**, 3143 (2000).

⁸S. Guha, S. B. Qadri, R. G. Musket, M. A. Wall, and T. Shimizu-Iwayama, *J. Appl. Phys.* **88**, 3954 (2000).

⁹R. Govindaraj, R. Kesavamoorthy, R. Mythili, and B. Viswanathan, *J. Appl. Phys.* **90**, 958 (2001).

¹⁰E. A. Irene, in *In Situ Real-Time Characterization of Thin Films*, edited by O. Auciello and A. R. Krauss (Wiley, New York, 2001), pp. 57–103.

¹¹R. M. A. Azzam and N. M. Bashara, *Ellipsometry and Polarized Light* (North-Holland, Amsterdam, 1977).

¹²C. C. Katsidis, D. I. Siapkas, A. K. Robinson, and P. L. F. Hement, *J. Electrochem. Soc.* **148**, G704 (2001).

¹³R. Tsu, D. Babić, and L. Ioriatti, Jr., *J. Appl. Phys.* **82**, 1327 (1997).

¹⁴D. R. Penn, *Phys. Rev.* **128**, 2093 (1962).

¹⁵C. Q. Sun, X. W. Sun, B. K. Tay, S. P. Lau, H. T. Huang, and S. Li, *J. Phys. D* **34**, 2359 (2001).

¹⁶V. Ranjan, M. Kapoor, and V. A. Singh, *J. Phys.: Condens. Matter* **14**, 6647 (2002).